中國機械工程學刊第四十四卷第五期第 455~462 頁(民國一百一十二年)
Journal of the Chinese Society of Mechanical Engineers, Vol.44, No.5, pp455~462 (2023)

On Semi-Automated Modeling of Systems with Friction for HiL-Simulation and Application to Electromechanical Actuators of Passenger Car

Zhenxing Ren and Jianfeng Guo

Keywords: Physical modeling, identification, data-driven modeling, PWA-model, Hardware-in-the-Loop-Simulation

ABSTRACT

Hardware-in-the-loop (HiL) simulation enables the development of electronic control units (ECUs) for automotive applications, requiring high-precision models to represent key components like electromechanical actuators. Most actuators incorporate significant friction, which is challenging to model. This paper proposes physical and data-driven modeling methods for electromechanical actuators. Both methods successfully achieved HiL simulation for functionally testing ECUs.

INTRODUCTION

Modern combustion engine research and development demands constant emissions, fuel consumption reductions, and improved performance. Satisfying these demands enables increasingly complex engine applications. If dynamic system models are available, efficient, model-based analysis and design procedures can be developed. A vital application is hardware-in-the-loop (HiL) simulation, providing a simulated driving environment enabling automatic testing of control devices in a virtual setting. The HiL environment allows testing in extreme conditions without real-world risks, including variable-speed simulation. Modeling reportedly comprises 50-90% of implementing model-based control systems (Kroll, 2016), which motivates semi-automated modeling method development.

Two approaches exist to achieve mathematical models of dynamic processes: theoretical or physical modeling versus data-driven modeling. Model structure and parameters are determined using physical principles or prior knowledge for physical modeling. Unknown parameters are set through experimentation. However, modeling systems with friction is typically challenging and resource-intensive, motivating algorithm development and enabling automated or semi-automated dynamic model identification.

Substantial work exists regarding friction description and modeling (Armstrong-Héouvry et al., 1994; Wit et al., 1995; Olsson et al., 1998; Marques et al., 2016; Pennestri et al., 2016; Gagnon et al., 2020). Usually, static models derive from stationary speed-friction relationships. However, recent research shows that dynamic friction effects must be considered in model development. Therefore, various dynamic friction models have been proposed, differing from static models by incorporating static friction (e.g., adhesive, sliding, viscous) and dynamic effects like the Dahl effect. Many studies address electromechanical actuator physical modeling, facing principal challenges in unknown parameters from high non-linearity like friction. Formal modeling and friction identification can apply physical principles. While most accurately capture friction effects, some require detailed physics knowledge, expensive experiments (Nakada et al., 2005; Pavkovic et al., 2006; Grepl and Lee, 2010), or complex numerical methods (Nakano et al., 2006; Yuan et al., 2011).

For data-driven methods, the piecewise affine (PWA) models have gained interest recently due to their high approximation ability (Vaezi and Izadian, 2015). PWA models partition the regression space into polyhedral convex regions. Globally, PWA models approximate nonlinear systems; locally, mapping from regression to output is piecewise affine, enabling the direct application of linear theory. PWA models address challenging system analysis, prediction, simulation modeling, and control design problems (Breschi et al., 2016; Wang et al., 2020). Roll et al. (2004) identified PWA models using mixed-integer linear or quadratic programming, suitable only for limited data. Juloski et al. (2005)'s Bayesian method estimates model parameters as random variables but requires precise system knowledge. Ferrari-Trecate et al. (2003), Nakada et al. (2005), and Breschi et al. (2016) proposed clustering-based methods, classifying data into sub-models using clustering algorithms and

Paper Received April, 2023. Revised June, 2023. Accepted August, 2023. Author for Correspondence: Zhenxing Ren.

Lecturer, College of Data Science, Taiyuan University of Technology, Jinzhong, Shanxi, PRC.

estimating sub-model parameters and partition boundaries simultaneously or subsequently. However, design parameters must be tuned appropriately. Local parameters from least-squares methods minimizing least-mean-square errors for series-parallel models are generally biased, limiting prediction quality for parallel evaluation (e.g., simulation) (Kroll, 2016). Modification of these approaches is needed, especially for simulation systems with friction.

This paper proposes physical and data-driven methods for the semi-automated modeling of systems with friction. For physical modeling, simple physical principles inform model structure. Model parameters derive from input/output data in open-loop experiments. A novel clustering-based piecewise affine (PWA) method is proposed for data-driven modeling, requiring fewer design parameters and suited for large or non-Gaussian data sets. The number of sub-model is determined by minimizing the model prediction error. Bias-free parameter estimation employs parallel identification. Both approaches enabled hardware-in-the-loop simulation of electromechanical actuators for passenger cars.

METHODS

PROBLEM STATEMENT

Friction is a nonlinear, complex, stochastic phenomenon essential to developing electromechanical actuators. Typically arising from interactions between two surfaces, friction effects encompass adhesive traction, sliding, viscous friction, and more. Friction introduces complications, including asymmetry, stick-slip effects, variable adhesion, and other issues. Friction is also impacted by temperature, humidity, aging, and other factors, remaining challenging to comprehend and model (Marques, 2016; Gagnon, 2020; Simoni, 2020).

As a typical electromechanical actuator, a throttle (see Figure 1) primarily comprises a DC servo motor, a gearbox, a return spring, a potentiometer angle sensor, and a throttle plate. The DC servo motor actuates the throttle. The angle sensor generates an output signal ranging from 0.5-4.5V to indicate the throttle plate position. Friction arises primarily between gears and bearings/shafts within the gearbox. Physical models commonly represent friction as a nonlinear function of angular velocity.

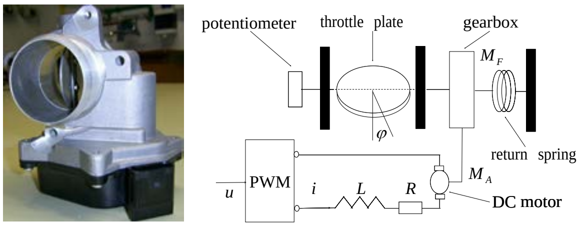

Fig. 1 A typical throttle and its technology scheme

In order to enable data collection for model identification, validation, and hardware-in-the-loop simulation, a test stand was constructed. Figure 2 provides a schematic illustration. The system incorporated National Instruments hardware for PWM control signal implementation and measurement data recording. A LabVIEW-based application program was developed to allow user operation of the test stand. Open-loop input/output measurement data was automatically recorded at a defined sampling rate.

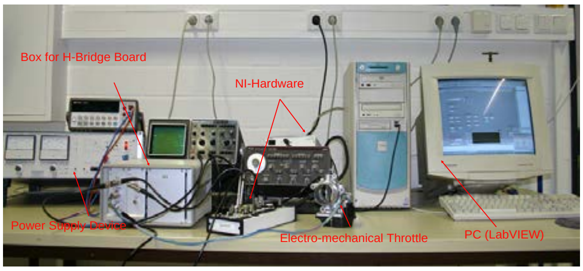

Fig. 2 Test stand

PHYSICAL MODELING

Typically, the physical model of the electromechanical throttle comprises a linear sub-model representing electromechanical components and a nonlinear sub-model for friction effects. Friction is defined as follows:

$$M_R = \begin{cases} M_A - M_F, \text{if } \dot{y} = 0 \text{ and } |M_A - M_F| \le M_H \\ M_G \cdot \operatorname{sgn}(\dot{\varphi}) + k_R \cdot \dot{\varphi}, \quad \text{otherwise} \end{cases} \tag{1}$$

$M_{.H.}$ is the static friction torque, $M_{.G.}$ is the Coulomb friction torque, and k_R is the viscosity coefficient. The DC servo motor can be defined by the following standard model: one equation for the motor current

$$i = \frac{1}{R} \cdot u - \frac{L}{R} \cdot \frac{\mathrm{d}i}{\mathrm{d}t} - \frac{k_M}{R} \cdot \dot{\varphi} \tag{2}$$

and one equation for the motor torque

$$M_A = k_M \cdot i \tag{3}$$

where u is the duty cycle, i is the current, R is the motor resistance, L is the motor inductance, and k_M is the motor constant. Since the dominant time constant $\tau = L/R$ is much smaller than the sampling time T_S, the dynamics of the DC servo motor can be neglected, and (2) and (3) can be simplified and combined to:

$$M_A = k_M \cdot i = \frac{k_M}{R} \cdot u - \frac{k_M \cdot k_M}{R} \cdot \dot{\varphi} = k_V \cdot u - k_{EMF} \cdot \dot{\varphi} \tag{4}$$

with $k_V = k_M / R$ and $k_{EMF} = k_M \cdot k_M / R$. The return spring is utilized for safety reasons to pull the plate to the open position φ_o. The resulting spring torque is given by:

$$M_F = k_F \cdot (\varphi_o - \varphi) + M_o \tag{5}$$

where k_F is the spring stiffness and M_o is the spring torque at the open position φ_o. When combining all the torques mentioned above with the inertia torque $J \cdot \ddot{\varphi}$ and a duty-free assumption $(M_L = 0)$ for modeling, the model has the following form:

$$J \cdot \ddot{\varphi} = M_F - M_A + M_R + M_L$$
$$= \begin{cases} 0 & \text{if } \dot{\varphi} = 0 \text{ and } \left|k_V \cdot u - k_F \cdot (\varphi_o - \varphi) - M_o\right| \le M_H \\ k_F \cdot (\varphi_o - \varphi) + M_o - k_V \cdot u + k_{EMF} \cdot \dot{\varphi} & \\ + M_G \cdot \operatorname{sgn}(\dot{\varphi}) + k_R \cdot \dot{\varphi} & \text{otherwise} \end{cases} \quad (6)$$

$\Leftrightarrow$

$$\ddot{\varphi} = \begin{cases} 0 & \text{if } \dot{\varphi} = 0 \text{ and } \left|b_0 \cdot u - a_0 \cdot (\varphi_o - \varphi) - c_o\right| \le c_H \\ a_0 \cdot \varphi' + a_1 \cdot \dot{\varphi} + b_0 \cdot u + f & \text{otherwise} \end{cases} \quad (7)$$

with $\varphi' = \varphi_0 - \varphi$ and the affine term $f = c_0 + c_1 \cdot \operatorname{sgn}(\dot{\varphi})$. The unknown parameters in (7) are given as: $a_0 = k_F / J$, $a_1 = k_R + k_{EMF} / J$, $b_0 = -k_V / J$, $c_0 = M_0 / J$, $c_1 = M_G / J$ and $c_H = M_H / J$.

If the conditions $\dot{\varphi} = 0$ and $|M_A - M_F| \le M_H$ are met, the actuator may remain stationary due to static friction. For the following explanation, we assume this condition persists during transitions from stiction to sliding. As the actuator closes, the motor torque exceeds the spring torque. As it opens, the spring torque dominates the motor torque. Both processes are defined as follows:

$$\textbf{Closing:}\ M_A > M_F \Rightarrow \left|M_A - M_F\right| = M_A - M_F = M_H \quad (8)$$
$$\Leftrightarrow a_0 \cdot (\varphi_o - \varphi) + b_0 \cdot u + c_0 = c_H$$

$$\textbf{Opening:}\ M_A < M_F \Rightarrow \left|M_A - M_F\right| = -(M_A - M_F) = M_H \quad (9)$$
$$\Leftrightarrow a_0 \cdot (\varphi_o - \varphi) + b_0 \cdot u + c_0 = -c_H$$

The continuous movement of the throttle in both processes can also be described by:

$$\textbf{Closing:}\ \dot{\varphi} < 0 \Rightarrow \operatorname{sgn}(\dot{\varphi}) = \text{-}1$$
$$\Rightarrow \ddot{\varphi} = a_0 \cdot (\varphi_o - \varphi) + a_1 \cdot \dot{\varphi} + b_0 \cdot u + c_0 - c_1 \quad (10)$$

$$\textbf{Opening:}\ \dot{\varphi} > 0 \Rightarrow \operatorname{sgn}(\dot{\varphi}) = 1 \quad (11)$$
$$\Rightarrow \ddot{\varphi} = a_0 \cdot (\varphi_o - \varphi) + a_1 \cdot \dot{\varphi} + b_0 \cdot u + c_0 + c_1$$

In the transition phase from sliding to stiction, the velocity is relatively small ($\dot{\varphi} \approx 0$ and $\ddot{\varphi} = 0$), therefore (10) and (11) can be rewritten as:

$$\textbf{Closing:}\ a_0 \cdot (\varphi_o - \varphi) + b_0 \cdot u + c_0 = c_1 \quad (12)$$

$$\textbf{Opening:}\ a_0 \cdot (\varphi_o - \varphi) + b_0 \cdot u + c_0 = -c_1 \quad (13)$$

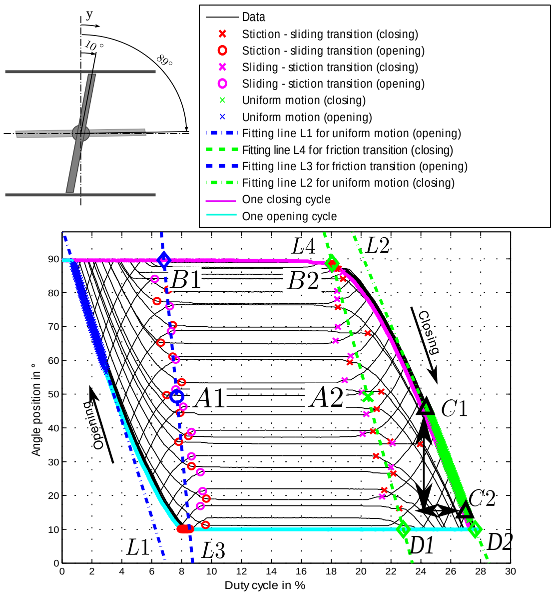

Fig. 3 Input/output characteristic of measurement with four fitting lines and particular points for identification

As mentioned, the model parameters will be obtained in the following steps. In the first step, $a_0/b_0, a_1/b_0, c_0/b_0, c_1/b_0$ and c_H/b_0 can be determined from the input/output characteristic, which results from a triangle-shaped test signal. Fig. 3 shows four *L1*~ *L4* fitting lines (*L1* for the uniform opening motion, *L2* for the uniform closing motion, *L3* for the transition from stiction to sliding, and *L4* for the transition from sliding to stiction) and particular points A_1~ D_2. *L1*~ *L4* were determined based on the measurement data using the RANSAC algorithm (Zuliani et al., 2003). The particular points A_1~ D_2 on fitting lines are used to estimate unknown parameters with the following relationships:

$$\frac{a_0}{b_0}: (10)|_{A1} - (10)|_{B1} \Rightarrow a_0 \cdot (\varphi_{B1} - \varphi_{A1}) + a_1 \cdot (\dot{\varphi}_{A1} - \dot{\varphi}_{B1}) + b_0 \cdot (u_{A1} - u_{B1}) = 0 \quad (14)$$
$$\text{with } \dot{\varphi}_{A1} = \dot{\varphi}_{B1} \quad \Rightarrow \frac{a_0}{b_0} = \frac{u_{A1} - u_{B1}}{\varphi_{A1} - \varphi_{B1}}$$

$$\frac{a_1}{b_0}: (10)|_{A2} - (12)|_{B2} \Rightarrow \ddot{\varphi}_{A2} = a_0 \cdot (\varphi_{B2} - \varphi_{A2}) + a_1 \cdot \dot{\varphi}_{A2} + b_0 \cdot (u_{A2} - u_{B2}) \quad (15)$$
$$\text{with } \varphi_{A2} = \varphi_{B2} \quad \Rightarrow \ddot{\varphi}_{A2} = a_1 \cdot \dot{\varphi}_{A2} + b_0 \cdot (u_{A2} - u_{B2})$$
$$\text{with } \dot{\varphi}_{A2} = const. \quad \Rightarrow -\frac{a_1}{b_0} = \frac{u_{A2} - u_{B2}}{\dot{\varphi}_{A2}}$$

$$\frac{c_0}{b_0}: (8)|_{A3} + (9)|_{B3} \quad \Rightarrow a_0 \cdot (\varphi_o - \varphi_{A3}) + a_0 \cdot (\varphi_o - \varphi_{B3}) + b_0 \cdot (u_{A3} + u_{B3}) + 2 \cdot c_0 = 0 \quad (16)$$
$$\text{with } \varphi_{A3} = \varphi_{B3} = \varphi_o \quad \Rightarrow -\frac{c_0}{b_0} = \frac{u_{A3} + u_{B3}}{2}$$

$$\frac{c_1}{b_0}:(12)|_{A4}-(13)|_{B4}\Rightarrow a_0\cdot(\varphi_{B4}-\varphi_{A4})+b_0\cdot(u_{A4}-u_{B4}) = 2\cdot c_1 \tag{17}$$

$$\text{with } \varphi_{A4}=\varphi_{B4} \qquad \Rightarrow \frac{c_1}{b_0}=\frac{u_{A4}-u_{B4}}{2}$$

$$\frac{c_H}{b_0}:(8)|_{A5}-(9)|_{B5}\Rightarrow a_0\cdot(\varphi_{B5}-\varphi_{A5})+b_0\cdot(u_{A5}-u_{B5}) = 2\cdot c_H \tag{18}$$

$$\text{with } \varphi_{A5}=\varphi_{B5} \qquad \Rightarrow \frac{c_H}{b_0}=\frac{u_{A5}-u_{B5}}{2}$$

After rewriting (7), it follows as:

$$\ddot{\varphi}=\begin{cases}0 & \text{if } \dot{\varphi}=0 \text{ and} \left|u-\frac{a_0}{b_0}\cdot\varphi'-\frac{c_0}{b_0}\right|\le\frac{c_H}{b_0} \\ b_0\cdot\left[\frac{a_0}{b_0}\cdot\varphi'+\frac{a_1}{b_0}\cdot\dot{\varphi}+u+\frac{c_0}{b_0}+\frac{c_1}{b_0}\cdot\operatorname{sgn}(\dot{\varphi})\right] & \text{otherwise}\end{cases} \tag{19}$$

In order to estimate the rest parameter b_0, $\ddot{\varphi}$ should not be equal to 0. In the first step, the test signal with lower bandwidth drove the actuator. With this signal, the dynamics, like the system's second-order mode, cannot be sufficiently excited, and reliable estimation of b_0 cannot be reached. Therefore, a further step is needed to determine b_0 under $\ddot{\varphi}\neq 0$. Using the test signal with higher bandwidth, the higher system order can be sufficiently excited, and b_0 can be estimated using numerical optimization. The identification problem can be solved by minimizing the following cost function:

$$b_{0,opt}=\arg\min_{b_0}\frac{1}{N}\sum_{k=1}^{N}\left[\varphi_{Sim}(k,b_0)-\varphi_{Meas}(k)\right]^2 \tag{20}$$

PWA MODELING

Piecewise affine (PWA) modeling is widely applied, especially for hybrid systems such as switched systems. This study employs a typical PWA model structure, the PWARX (Piecewise AutoRegressive eXogenous) model, to represent electromechanical actuators. The model is defined as follows:

$$f(\boldsymbol{x}(k))=\begin{cases}\boldsymbol{\theta}_1^T\begin{bmatrix}\boldsymbol{x}(k)\\1\end{bmatrix} & \text{if } \boldsymbol{x}\in\boldsymbol{\chi}_1\\ \vdots & \\ \boldsymbol{\theta}_c^T\begin{bmatrix}\boldsymbol{x}(k)\\1\end{bmatrix} & \text{if } \boldsymbol{x}\in\boldsymbol{\chi}_c\end{cases} \tag{21}$$

with the regressor:

$$\boldsymbol{x}(k)=[y(k-1)\; y(k-2)\ldots y(k-n_a)\; u(k-1)\; u(k-2)\ldots u(k-n_b)]^T \tag{22}$$

where $u(k)\in\Re$ is the model input, n_a and n_b are the numbers of used past outputs and inputs, $n=n_a+n_b$. The regression space is split into c polyhedral partitions. $\{\chi_i\}_{i=1}^{c}$ is a polyhedral partition of the regression space, and $\boldsymbol{\theta}\in\Re^{n+1}$ is a parameter vector.

When applying clustering-based methods to identify systems exhibiting friction, particular attention must be paid to friction phenomena. The original regression model in Eq. (21) incorporates past inputs and outputs unsuitable for representing friction effects. Given the velocity-dependent features arising from friction, using $y(k-1)-y(k-2)$ and $u(k-1)$ as regressors is more reasonable. Because location-dependent effects were not observed in measurements, *y(k-1)* will be excluded. The standard k-means clustering algorithm will then be employed for clustering in the new regression space. Figure 4 depicts the allocation of measurement data given c = 8 clusters. Points in the regression space are labeled by cluster index following clustering, indicating velocity-dependent friction effects are well classified.

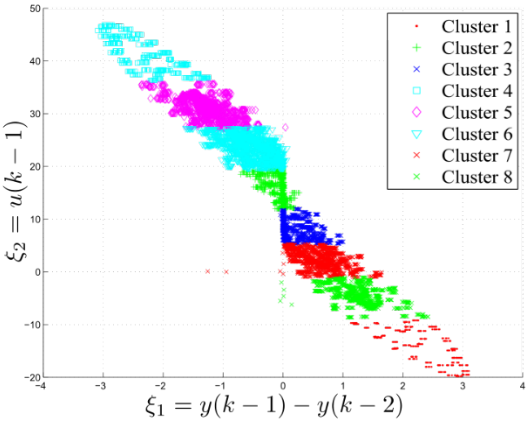

Fig. 4 Cluster result

Model parameters are then optimized through parallel identification because, as reported (Kroll, 2016), parallel identification can achieve a higher prediction quality. Initial parameter values for optimization are established using serial-parallel identification. Serial-parallel identification calculates output based on past inputs and outputs, which can be solvable by standard least squares methods. However, serial-parallel identification may produce biased parameters. In contrast, parallel identification calculated output based on past inputs and predicted outputs, which should be solved using optimization methods.

RESULTS AND DISCUSSIONS

As previously discussed, the model will undergo hardware-in-the-loop (HiL) simulation and must predict actuator output precisely to enable functional testing of electronic control units (ECUs). Two criteria were employed to evaluate model quality quantitatively:

$$\text{NRMSE}=\sqrt{\frac{\sum_{k=1}^{N}(y(k)-\hat{y}(k))^2}{\sum_{k=1}^{N}(y(k)-\bar{y})^2}} \tag{23}$$

$$\|e\|_\infty=\max_k(|\hat{y}(k)-y(k)|) \tag{24}$$

For this application, the specified requirements are model performance $\|e\|_\infty\le 5°$ and normalized root mean square error (NRMSE) value as low as possible. In addition to quantitative evaluation, qualitative assessment of time series data and histograms will be used for validation. Models must be validated using "fresh" measurement data not incorporated into the identification process. An amplitude-modulated multi-step signal (APRTS) will serve as the test signal. The case study applied Both proposed modeling methods to an electromechanical throttle. In order to determine the optimal number of sub-models for the PWA model, the k-Means clustering algorithm was initialized ten times for values between 2 to 10 sub-models. Based on the resulting model quality, c=8 sub-models were selected.

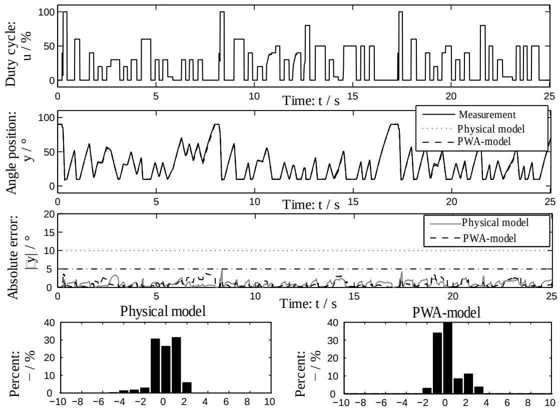

Fig. 5 Model predictions and measurements for parallel evaluation of both models

Table 1. Performance comparison of both models

Data type	Criterion	Physical model	PWA-model
Identification data	NRMSE	0.05	0.04
	$\|e\|_\infty$	4.21°	3.83°
Validation data	NRMSE	0.06	0.06
	$\|e\|_\infty$	4.93°	3.92°

The identified models will undergo parallel model evaluation, in which the model output depends on both the current input and past outputs. Comparing measurement and simulation results using new test data (see Fig. 5) shows that the model and actual system are highly similar. The model accurately reproduces friction behaviors such as static friction. However, the PWA model's residuals appear asymmetrically distributed in the histogram of Fig. 5. This asymmetry could be optimized by improving either the test signal design or model structure selection. Both modeling methods were quantitatively compared in Table 1. The maximum absolute error was 4.93° for the physical model and 3.92° for the PWA model. The normalized root mean square error (NRMSE) was 0.06° for both models. It means that the PWA model may provide superior model quality, with the potential to achieve the target of $\|e\|_\infty \leq 5°$.

The identified models have already been implemented on a microprocessor board to enable functional testing of the electronic control unit (ECU). The results are compared with measurement data (see Fig. 6).

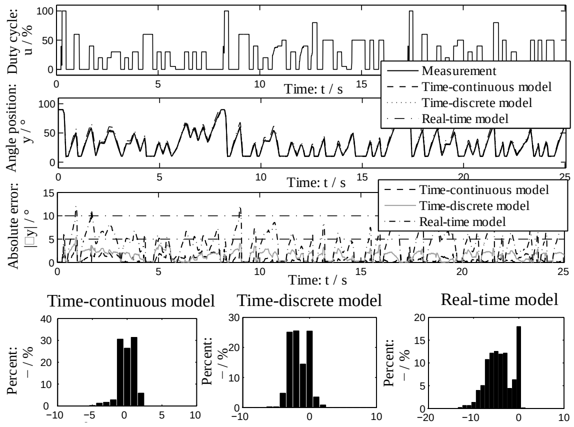

Fig. 6 Comparing different models with the measurement

A comparison of measurements and simulation in the open loop indicates that the hardware-in-the-loop (HiL) simulator can capture the real effects in principle. However, it is noted that there appears to be a visible deviation in the opening process. While the time-continuous model shows good consistency with the measurement data, the time-discrete simulation shows a deviation from the measurements, likely due primarily to discretization effects. Theoretically, the HiL simulator's hardware should reproduce the identified model, but Fig. 6 shows a more significant deviation. As Table 2 indicates, the error $\|e\|_\infty$ is about 12° for the HiL simulator, which exceeds the specified 5° limit. The coding of the implemented model on the microprocessor and electronic disturbances may account for this deviation. In order to compensate for the deviation, minor adjustments in the HiL simulator were carried out, and now the accurate electromechanical actuators can be replaced by the HiL-simulator for the functional testing of ECU.

Table 2. Performance comparison of different implementations

Criterion	Time-continuous model	Time-discrete model	Real-time model
NRMSE	0.06	0.07	0.12
$\|e\|_\infty$	4.93°	5.09°	12.08°

The presented modeling methods were also successfully applied to additional electromechanical actuators for passenger vehicles, such as swirl flaps, exhaust gas recirculation (EGR) valves, and electromagnetic valves, enabling real-time simulation. Therefore, the real-time simulator employing the proposed methods can be used for the hardware-in-the-loop (HiL) simulation of multiple electromechanical actuators.

Besides, both presented modeling methods are generally compared in Table 3.

Table 3. Performance comparison of different implementations

Aspect	Physical modeling	Data-driven modeling
Model type	Physical model	PWA-model
Prior knowledge	Medium	Little
Interpretability	Good	Limited
Extrapolability	Good	Limited
Prediction quality	Good	Very good
Transferability	Application specified	Universal

The physical modeling method employs natural and engineering principles based on necessary prior knowledge to develop differential equations describing the system. In contrast, the data-driven modeling method approximates the behavior of a nonlinear system based on limited prior knowledge. A typical data-driven model approximates a nonlinear system using a piecewise affine modeling method, which is achieved by composing affine and locally valid piecewise affine (PWA) sub-models as difference equations. Compared to the physical modeling approach, the PWA model can achieve a higher prediction accuracy when modeling complex electromechanical actuators, which tend to be more demanding to represent. However, the PWA model depicts only the target system's input-output transfer behavior.

Consequently, the resulting PWA model lacks a physical interpretation. Unlike physical models, PWA model parameters cannot be mapped to physical quantities in the system. Instead, they reflect complex statistical patterns rather than physical processes. The PWA model provides limited insight into the target system's inherent properties and dynamics since it produces statistical approximations tuned to the training dataset. Additionally, the PWA model has constrained extrapolability. Unlike physical models, data-driven models do not represent the causal factors or relationships governing the system's behavior. They detect input-output patterns but fail to capture deeper mechanisms. Thus, their predictions break down outside the range of common input-output pairs in the training data. It is challenging to determine the level of uncertainty in the model's predictions under new conditions starkly different from the training data, which makes uncertainty analysis difficult.

Overall, the presented modeling methods adequately capture the behavior of electromechanical actuators, producing model quality sufficient for hardware-in-the-loop (HiL) simulation and functional testing of electronic control units (ECUs). Both methods are efficient, relying on a few design parameters, allowing a model to be semi-automated and developed within 5 minutes.

CONCLUSIONS

This paper presented two semi-automated modeling approaches employing physical and data-driven identification methods for friction systems. Both approaches were applied to electromechanical actuators in passenger vehicles. Results indicate that both modeling approaches can efficiently yield models achieving performance $\|e\|_\infty \leq 5°$, adequate for hardware-in-the-loop simulation and functional electronic control unit testing. Further research will target improved test signal design and model-based controller development.

ACKNOWLEDGMENT

This research is supported by National Natural Science Foundation of China (Grant No. 12204345), Natural Science Foundation of Shanxi Province, China (Grant No. 20210302123188), and Natural Science Foundation for Young Scientists of Shanxi Province, China (Grant No. 202103021223107). The authors would like to thank anonymous reviewers for carefully reading the paper.

REFERENCES

Armstrong-Héouvry, B., Dupont, P., Wit, C.D., "A survey of models, analysis tools and compensation methods for control of machines with friction," *Automatica*, Vol. 30, pp.1038-1138 (1994).

Breschi, V., Piga, D., Bemporad, A., "Piecewise affine regression via recursive multiple least squares and multicategory discrimination," *Automatica*, Vol. 73, pp. 155–162 (2016).

Ferrari-Trecate, G., Muselli, M., Liberati, D., Morari, M., "A clustering technique for the identification of piecewise affine systems," *Automatica*, Vol. 39 pp. 205–217 (2003).

Gagnon, L., Morandini, M., Ghiringhelli, G. L., "A review of friction damping modeling and testing," *Arch Appl Mech*, Vol. 90, pp. 107–126 (2020).

Grepl, R., Lee, B., "Modeling, parameter estimation and nonlinear control of automotive electronic throttle using a rapid-control prototyping technique," *Experimental Techniques*, Vol. 11, pp. 601–610 (2010).

Juloski, A., Weiland, S., Heemels, W. P. M. H., "A bayesian approach to identification of hybrid systems," *IEEE Transactions on Automatic Control*, Vol. 50, pp. 1520–1533 (2005).

Kroll, A., *Computational Intelligence: Methods and Technical Applications*, De Gruyter Oldenbourg, London (2016).

Marques, F., Flores, P., Claro, J. C. P., Lankarani, H. M., "A survey and comparison of several friction force models for dynamic analysis of multibody mechanical systems," *Nonlinear Dynamics*, Vol. 86, pp. 1407–1443 (2016).

Nakada, H., Takaba, K., Katayama, T., "Identification of piecewise affine systems based on statistical clustering technique," *Automatica*, Vol. 41, pp. 905–913 (2005).

Nakano, K., Sawut, U., Higuchi, K., Okajima, Y., "Modeling and observer-based sliding-mode control of electronic throttle systems," *ETCI Transactions on Electrical Engineering, Electronics, and Communications*, Vol. 4, pp. 22–28 (2006).

Olsson, H., Åström, K.J., Wit, C.D., Gävert, M., Lischinsky, P., "Friction models and friction compensation," *European Journal of Control*, Vol. 4 pp.176–195 (1998).

Pavkovic, D., Deur, J., Jansz, M., Peri, N., "Adaptive control of automotive electronic throttle," *Control Engineering Practice*, Vol. 14, pp. 121–136 (2006).

Pennestri, E., Rossi, V., Salvini, P., Valentini, P. P., "Review and comparison of dry friction force models," *Nonlinear Dynamics*, Vol. 83, pp. 1785–1801 (2016).

Roll, J., Bemporad, A., Ljung, L., "Identification of piecewise affine systems via mix-integer programming", *Automatica*, Vol. 40, pp. 37–50 (2004).

Simoni, L., Beschi, M., Visioli, A., K. J. Åström, "Inclusion of the dwell time effect in the LuGre friction model," *Mechatronics*, Vol. 66, pp. 102345 (2020).

Vaezi, M., Izadian, A., "Piecewise affine system identification of a hydraulic wind power transfer system," *IEEE Transactions on Control Systems Technology*, Vol. 23 pp. 2077–2086 (2015).

Wang, J., Song, C., Zhao, J., Xu, Z., "A pwa model identification method for nonlinear systems using hierarchical clustering based on the gap metric, Computers and Chemical Engineering", Vol. 138, pp. 106838 (2020).

Wit, C.D., Olsson, H., Åström, K.J., P. Lischinsky, P., "A new model for control of systems with friction," *IEEE Transaction on Automatic Control*, Vol. 40, pp. 1189-1190 (1995).

Yuan, X. F., Li, T., Wang, Y. N., Sun, W., Wu, L.H., "Parameter identification of electronic throttle using a hybrid optimization algorithm," *Nonlinear Dynamics*, Vol. 63, pp. 549–557 (2011).

Zuliani, M., Kenney, C., Manjunath, B., "The multiransac algorithm and its application to detect planar homographie," Proc. of IEEE International Conference on Image Processing, Genova, Italy, (2005).

NOMENCLATURE

c	Number of clusters
i	Current
J	Inertia
k_F	Spring stiffness
k_M	Motor constant
k_R	Viscosity friction coefficient
k_{EMK}	Coefficient of back EMF
M_G	Coulomb friction moment
M_H	Static friction moment
M_o	Spring torque at the open position
M_R	Friction moment
M_{ext}	External moment
n_a	Number of past outputs
n_b	Number of past inputs
R	Resistance
T_A	Sampling time
u	Duty cycle
X(k)	Regressor vector
φ	Angular position
φ_o	The open position of the throttle plate
$\dot{\varphi}$	Angular velocity
$\ddot{\varphi}$	Angular acceleration
χ	Polyhedral partition
θ	Parameter vector

摩擦系統的半自動化建模及其在乘用車機電執行機構中的應用

任振興　　郭劍鋒
太原理工大學大數據學院

摘 要

在汽車應用中，特別是在電子控制單元(ECU)的開發中，硬件在環(HiL)發揮著重要的作用，這就要求高精度的模型來模擬車輛的機電執行器等關鍵部件。大多數執行器都是具有顯著摩擦效應的系統，對此類系統進行建模並非易事。本文提出了機電執行器的物理建模方法和數據驅動建模方法，並將這兩種方法應用於電控單元功能測試的 HiL 仿真。結果表明，這兩種方法都能有效地實現提供了高質量的模型，可以滿足 HiL 中 ECU 的功能測試模擬。